Probing the anomalous top quark couplings to the photon at future $e^{-}p$ colliders.

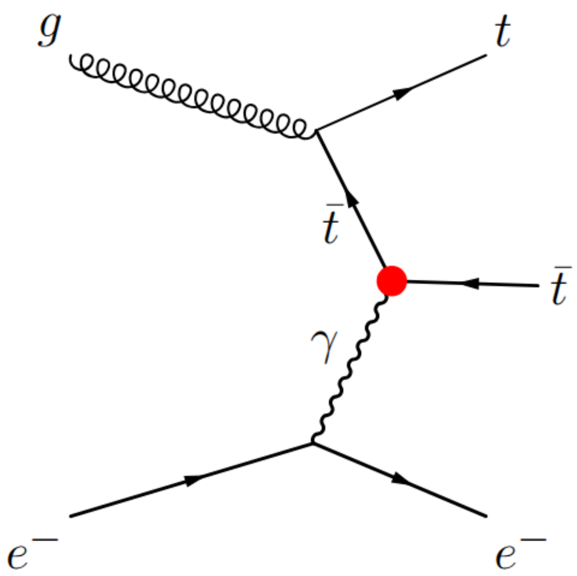

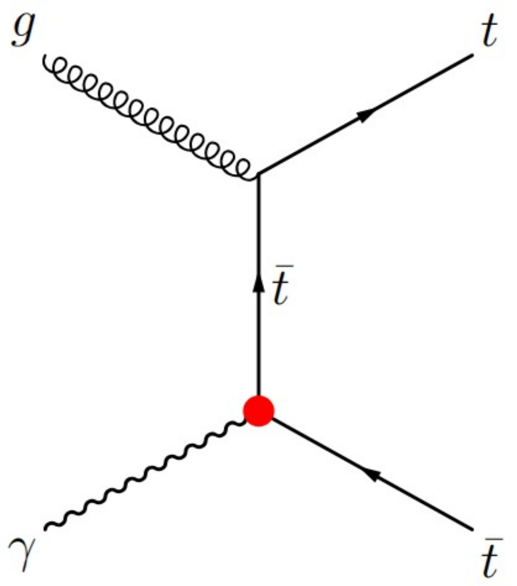

Mukesh Kumar

In collaboration with: Katlego Machethe

UNIVERSITY OF THE WITWATERSRAND, JOHANNESBURG

INSTITUTE FOR COLLIDER PARTICLE PHYSICS
UNIVERSITY OF THE WITWATERSRAND

❑ Top Quark: A Unique Probe

- Heaviest Standard Model particle ($m_t \approx 173$ GeV)
- Strongly coupled to the Higgs ($y_t \approx 1$) → sensitive to EWSB
- Decays before hadronizing → preserves spin info
- Potential window to new physics: compositeness, top partners, etc.

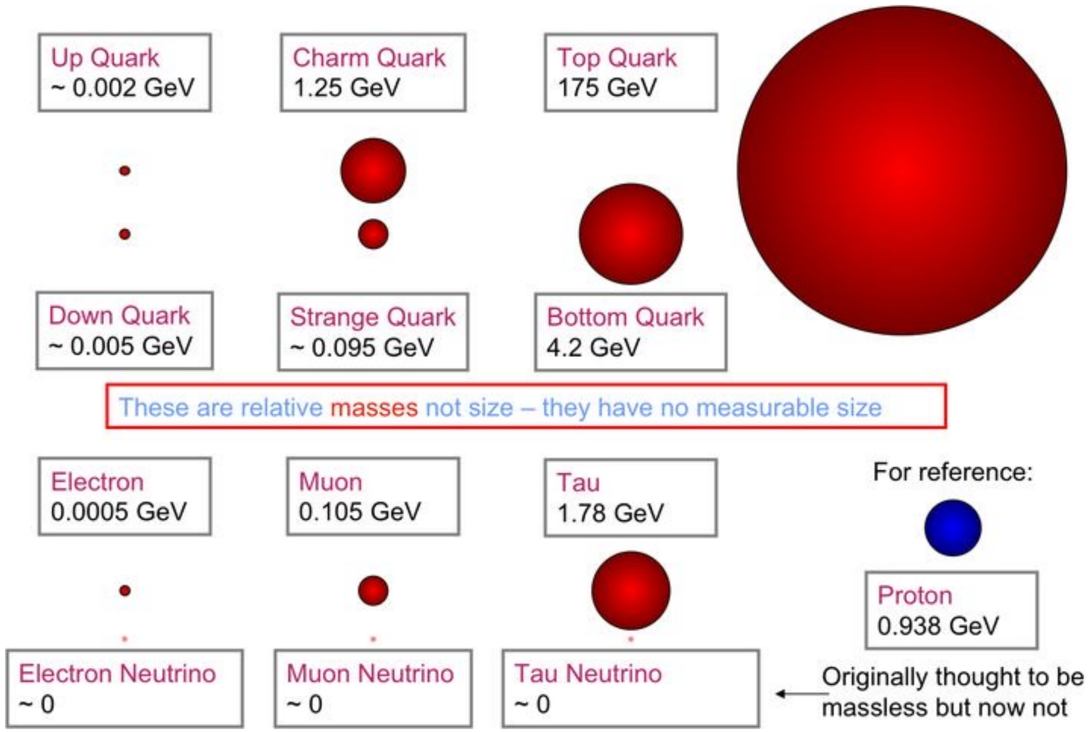

❑ Top-quark Coupling: A Key Vertex

- Direct probe of top-quark electroweak interactions
- Sensitive to BSM effects via anomalous couplings (vector, axial, dipole)
- Affects Higgs production, EW symmetry, and top-quark compositeness
- Complementary to $Wtb, t\bar{t}V$ $(V = \gamma, Z, h)$, and EFT global fits..

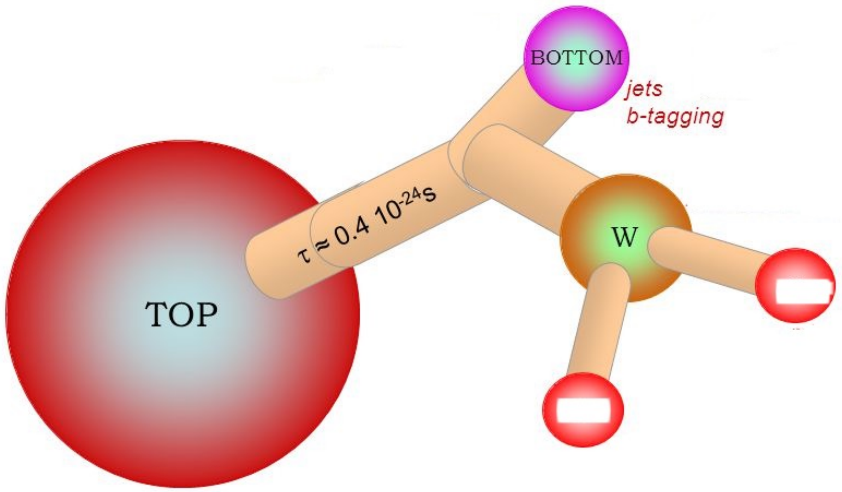

$$t \to W^+ b \left(\bar{t} \to W^- \bar{b}\right);\ W^\pm \to \ell^\pm \nu_\ell / jj$$

❑ Why e^-p Collider for $t\bar{t}\gamma$?

- ➢ Clean initial state (lepton-proton) → reduced QCD background
- ➢ Enhanced sensitivity to neutral current processes
- ➢ Direct access to $e^-p \to t\bar{t}e^-$ via γ exchange OR photo-production: $\gamma p \to t\bar{t}$
- ➢ Less ambiguous interpretation than pp; polarized beams possible
- ➢ Ideal for disentangling EFT operators in $t\bar{t}\gamma$ vertex

The interaction for the $t\bar{t}\gamma$ vertex is:

$$\mathcal{L}_{t\bar{t}\gamma} = \left[-eQ_t\bar{t}\gamma^\mu(1+\Delta C_V)tA_\mu\right]$$

$$+ \left[-e\bar{t}\frac{i\sigma^{\mu\nu}q_\nu}{m_t}(d_V+id_A)tA_\mu\right]$$

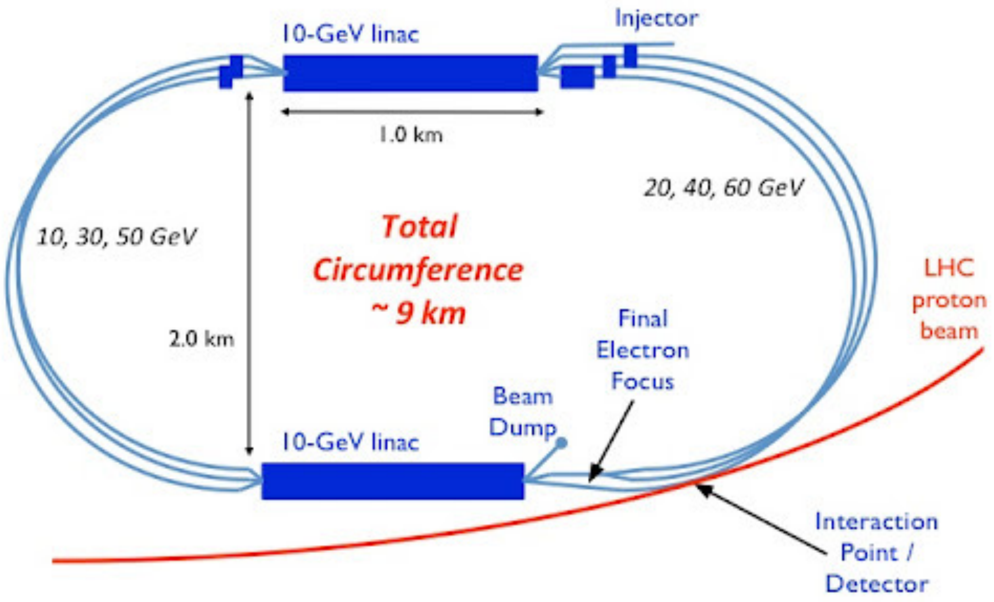

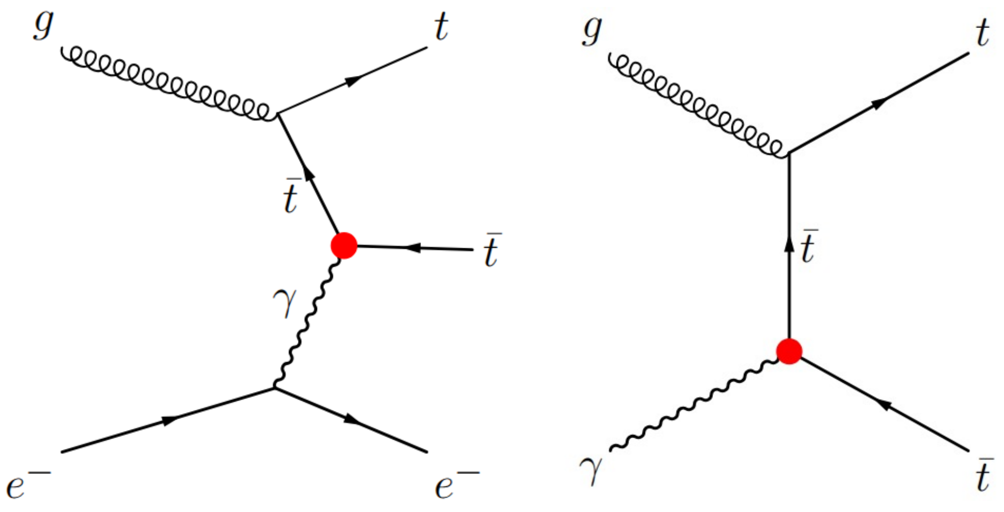

Cross section(s) studies:

❖ The $t\bar{t}\gamma$ couplings at $e^{-}p$

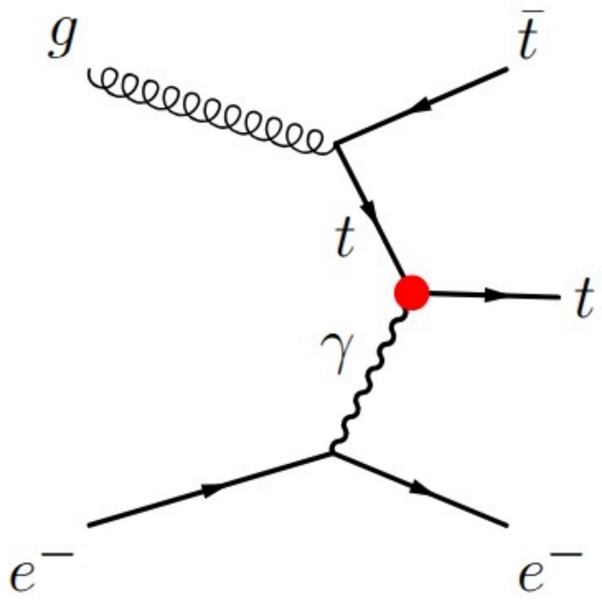

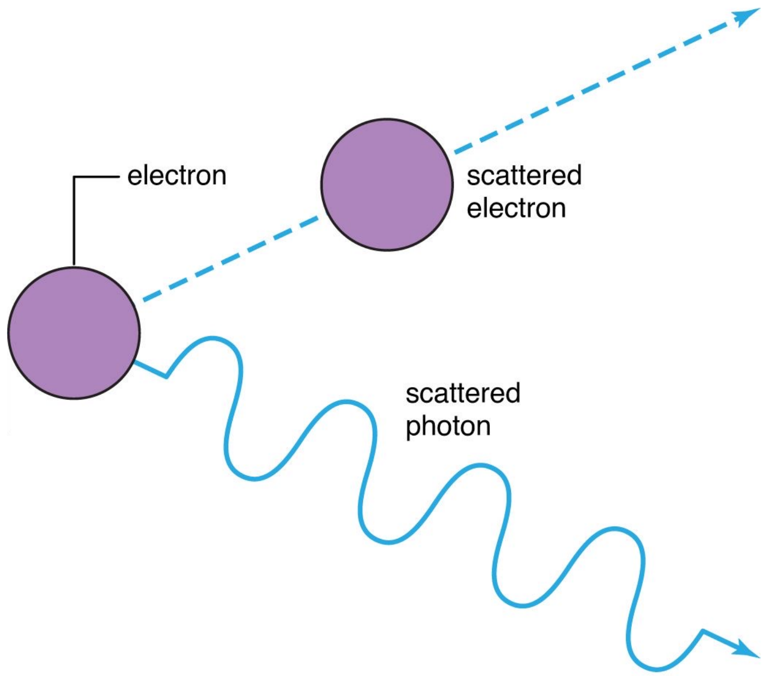

Photoproduction

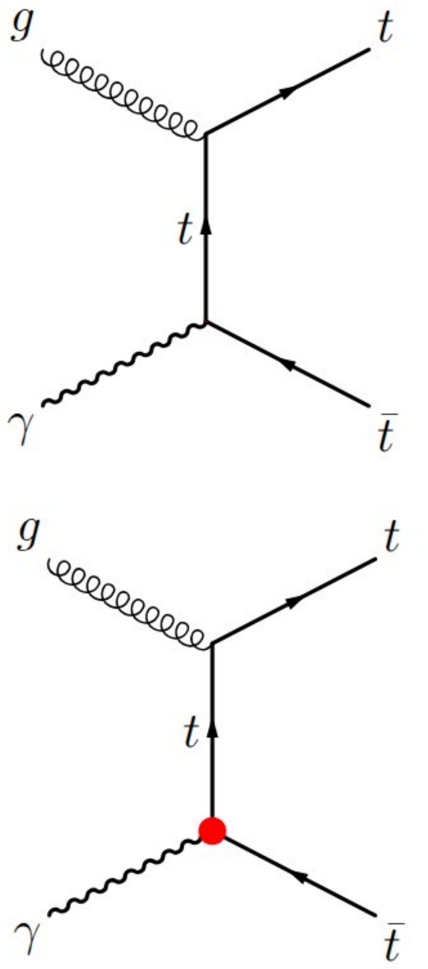

Final state	σ(fb)
Hadronic	3.56
Semi-leptonic	2.36
Di-leptonic	0.39

Final state	σ(fb)
Semi-leptonic	12.92
Hadronic	19.37
Di-leptonic	2.16

Cross section(s) studies in photo-production: $\gamma p \to t\bar{t}$ **[semi-leptonic top-decay]**

$t \to W^+ (\to \ell^+\nu_\ell/jj)b$ $\bar{t} \to W^- (\to jj/\ell^-\nu_\ell)b^-$ $\ell^\pm = e^\pm, \mu^\pm$

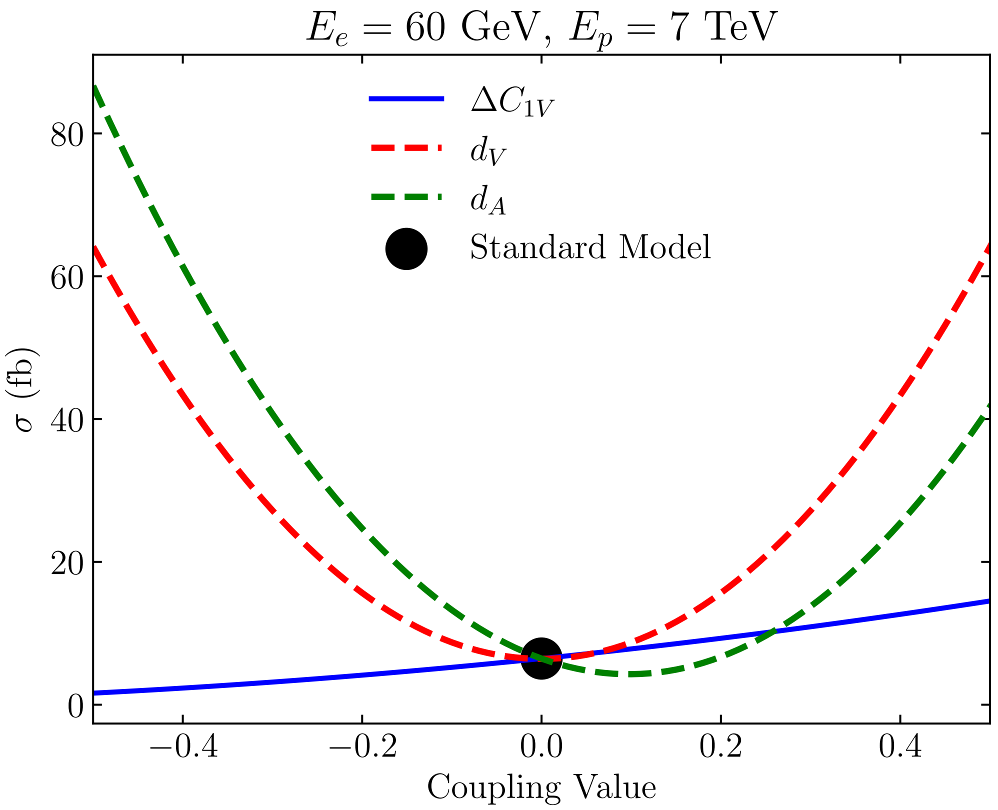

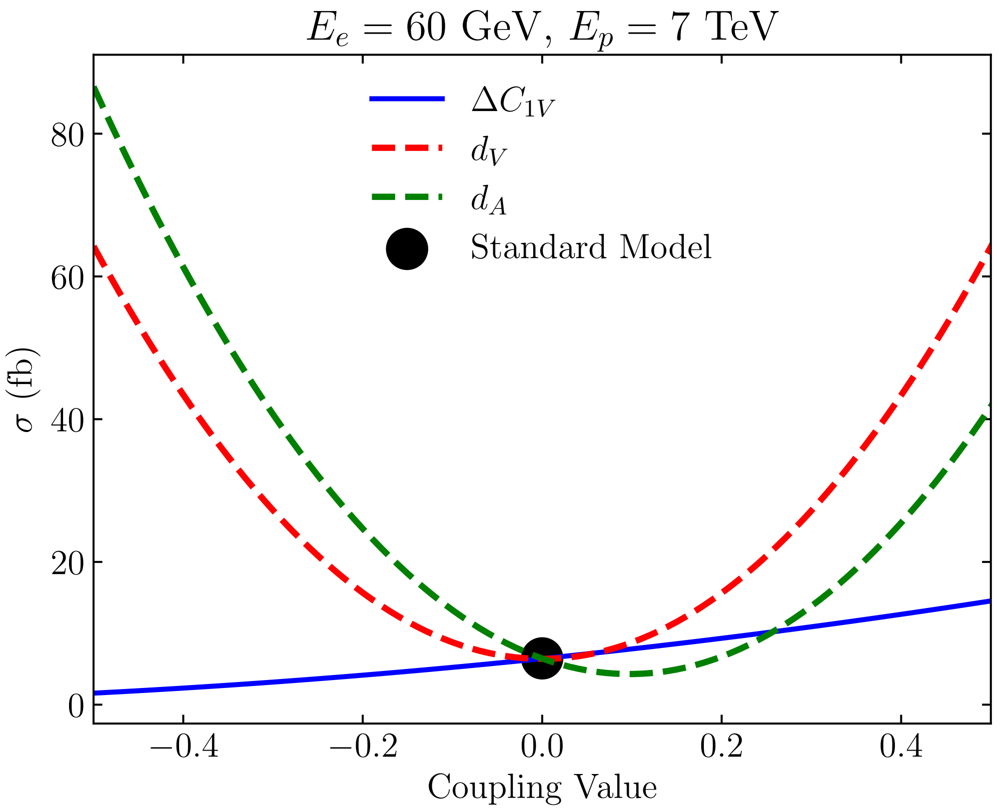

Cross section(s) studies: photo-production: $\gamma p \to t\bar{t}$ **[hadronic & di-leptonic top-decay]**

$t \to W^+ (\to \ell^+ \nu_\ell / jj) b$ $\quad$ $\bar{t} \to W^- (\to jj / \ell^- \nu_\ell) b^-$ $\quad$ $\ell^\pm = e^\pm, \mu^\pm$

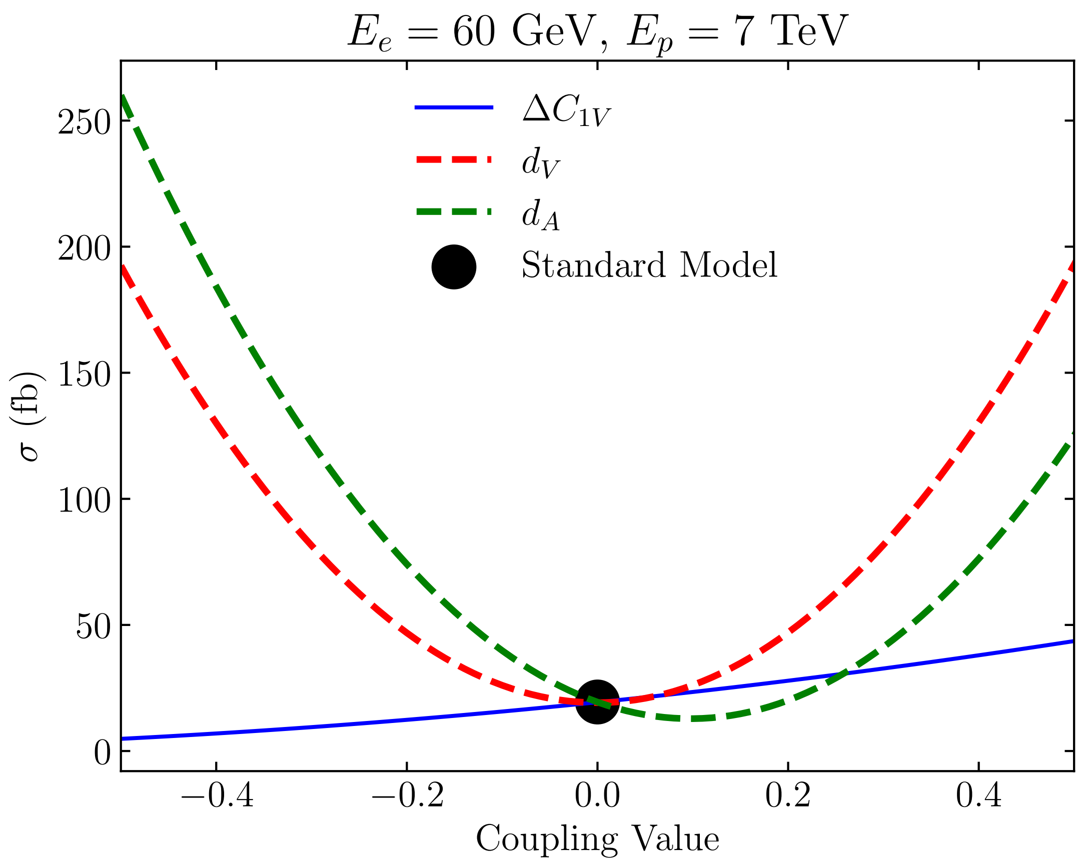

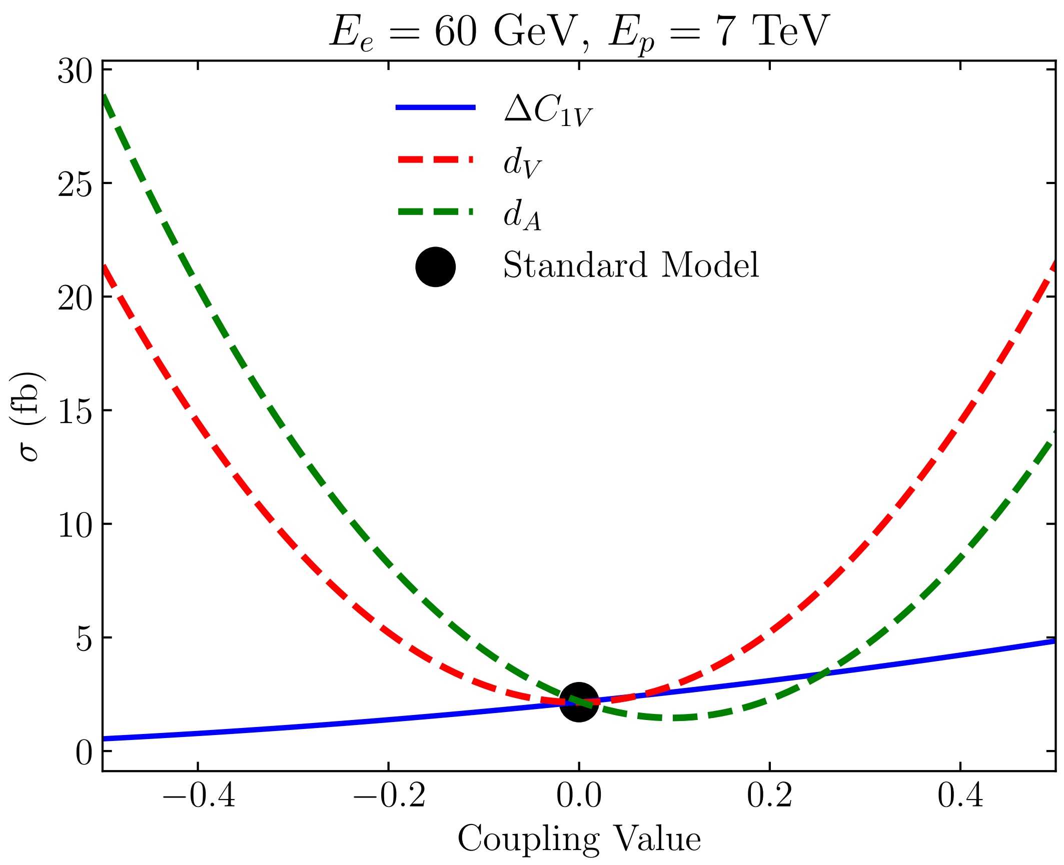

Significance studies:

photo-production: $\gamma p \to t\bar{t}$ **[di-leptonic & semi-leptonic top-decay]**

TABLE II. Cutflow for the SM signal and dominant backgrounds normalized to the luminosity $\mathcal{L} = 50$ (1000) fb^{-1}, and assuming a b-tagging efficiency of 70% for the di-leptonic and semi-leptonic final states. The optimized selection cuts considered are: (a) 150 GeV $< m_{bjj} <$ 200 GeV, and $m_{b\ell^+/\bar{b}\ell^-} <$ 170 GeV for the semi-leptonic final state, and (b) $m_{b\ell^+/\bar{b}\ell^-} <$ 170 GeV for the di-leptonic final state. The local significance $N_{\rm SD}$ with a systematic uncertainty of $\delta_s = 5\%$ for the SM signal and backgrounds is shown in the last row.

	Di-leptonic		Semileptonic (ℓ^-)		Semileptonic (ℓ^+)	
	Generation level	Optimized	Generation level	Optimized	Generation level	Optimized
SM signal	75.3(1505.3)	64.4(1288.8)	226.3(4526.2)	193.6(3872.9)	226.1(4521.1)	193.9(3877.1)
Background	44.3(886)	7.73(154.8)	135(2699.4)	14.8(296)	134.6(2691.3)	15.5(310.7)
N_{SD}	6.4(15)	7.1(17.1)	9.8(16.3)	11.1(18.9)	9.8(16.4)	11.1(18.9)

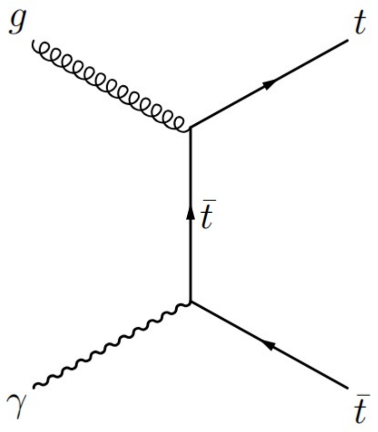

$$N_{\rm SD} = S/\sqrt{S + B + (\delta_S \cdot S)^2 + (\delta_S \cdot B)^2}$$

Sensitive Observable(s):

photo-production: $\gamma p \to t\bar{t}$ **[di-leptonic top-decay]**

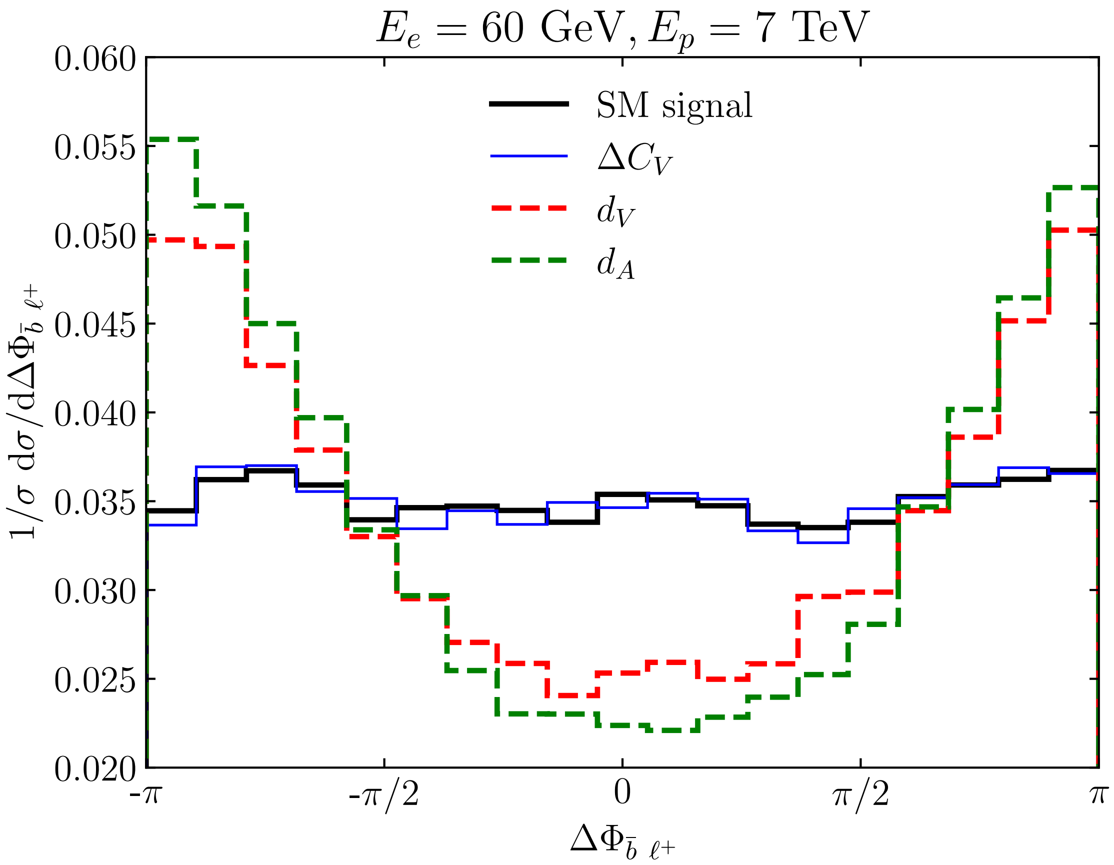

Analysis and Results:

The χ^2 is defined as

$$\chi^2 = \sum_{k=1}^{n} \left(\frac{\sigma_k^{\mathrm{BSM}}(C_i) - \sigma_k^{\mathrm{exp}}}{\Delta\sigma_k} \right)^2 ,$$

$$\Delta\sigma_k = \sqrt{\frac{\sigma_k^{\mathrm{SM+Bkg}}}{\mathcal{L}} + \left(\delta_s \sigma_k^{\mathrm{SM+Bkg}}\right)^2} .$$

The dependence of the inclusive and differential cross sections on the BSM couplings can be modelled as a quadratic function:

$$\sigma^{\mathrm{BSM}}(C_i) = \sigma^{\mathrm{SM}} + \sum_i C_i A_i + \sum_{i,j} C_i C_j B_{ij} ,$$

Analysis and Results:

photo-production: $\gamma p \to t\bar{t}$ **[di-leptonic top-decay]**

$$\mathcal{L}_{t\bar{t}\gamma} = \left[-eQ_t\bar{t}\gamma^{\mu}(1+\Delta C_V)tA_{\mu}\right]$$

$$+\left[-e\bar{t}\frac{i\sigma^{\mu\nu}q_{\nu}}{m_t}(d_V+id_A)tA_{\mu}\right]$$

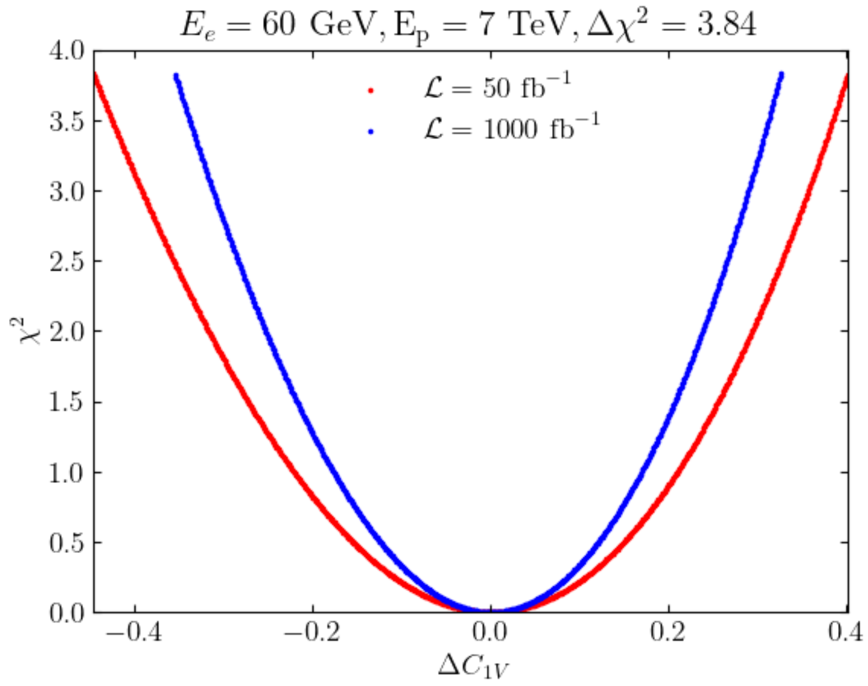

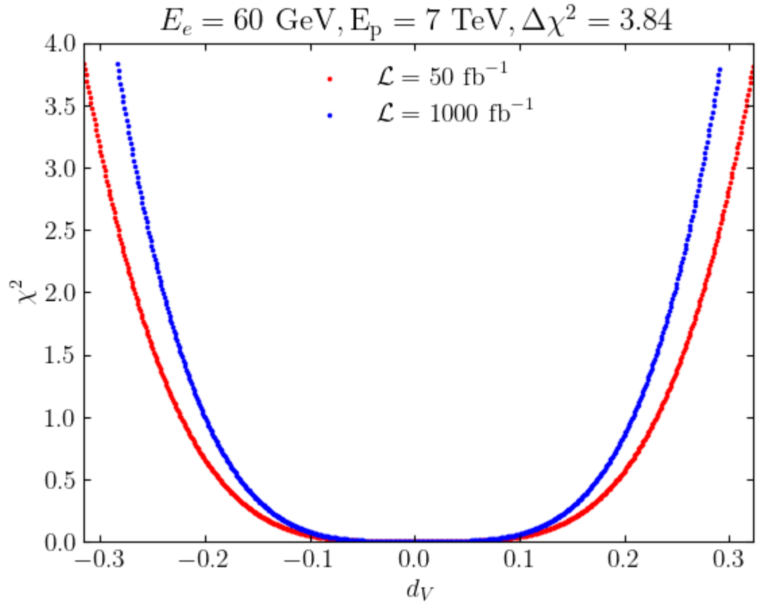

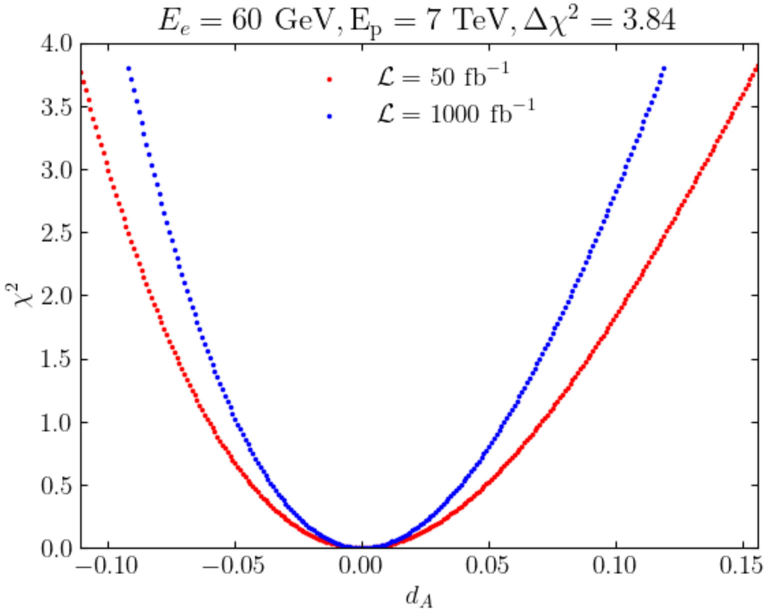

The χ^2 is defined as

$$\chi^2 = \sum_{k=1}^{n}\left(\frac{\sigma_k^{\rm BSM}(C_i)-\sigma_k^{\rm exp}}{\Delta\sigma_k}\right)^2,$$

Sensitive Observable(s): photo-production: $\gamma p \to t\bar{t}$ **[semi-leptonic top-decay]**

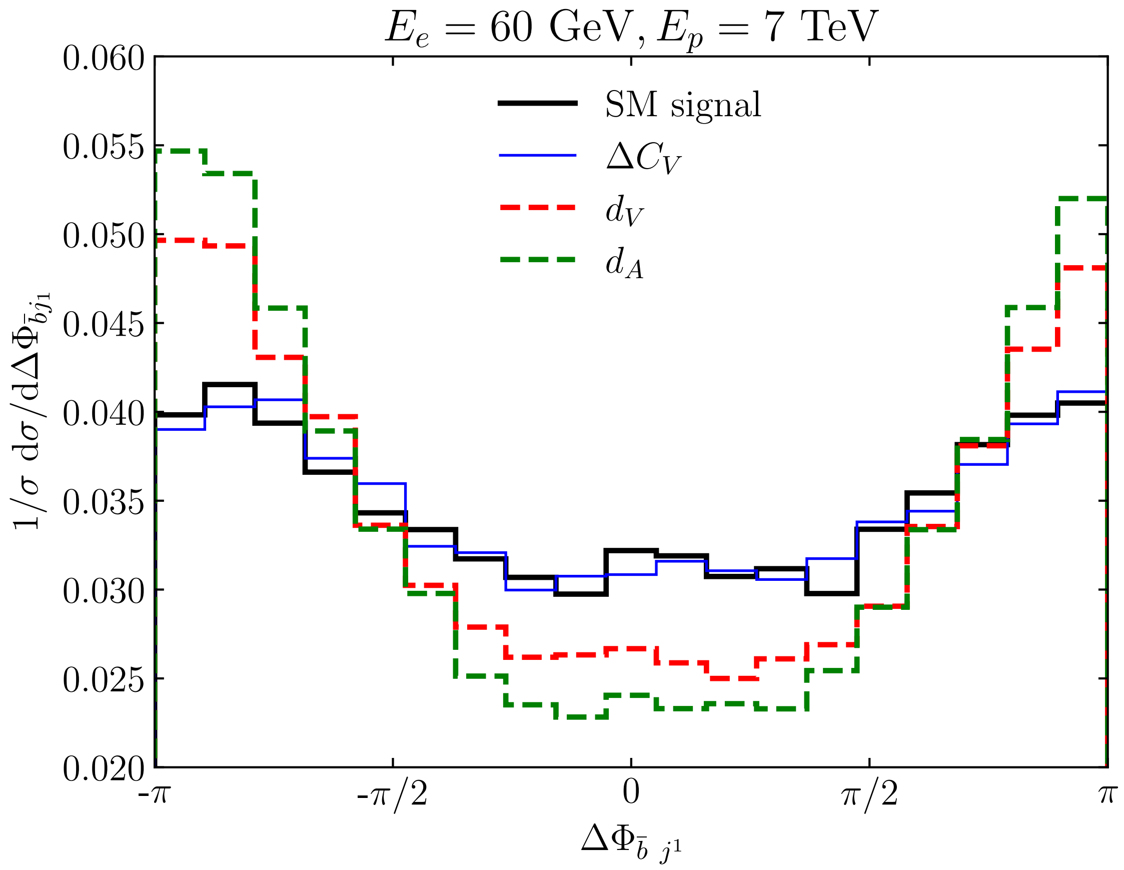

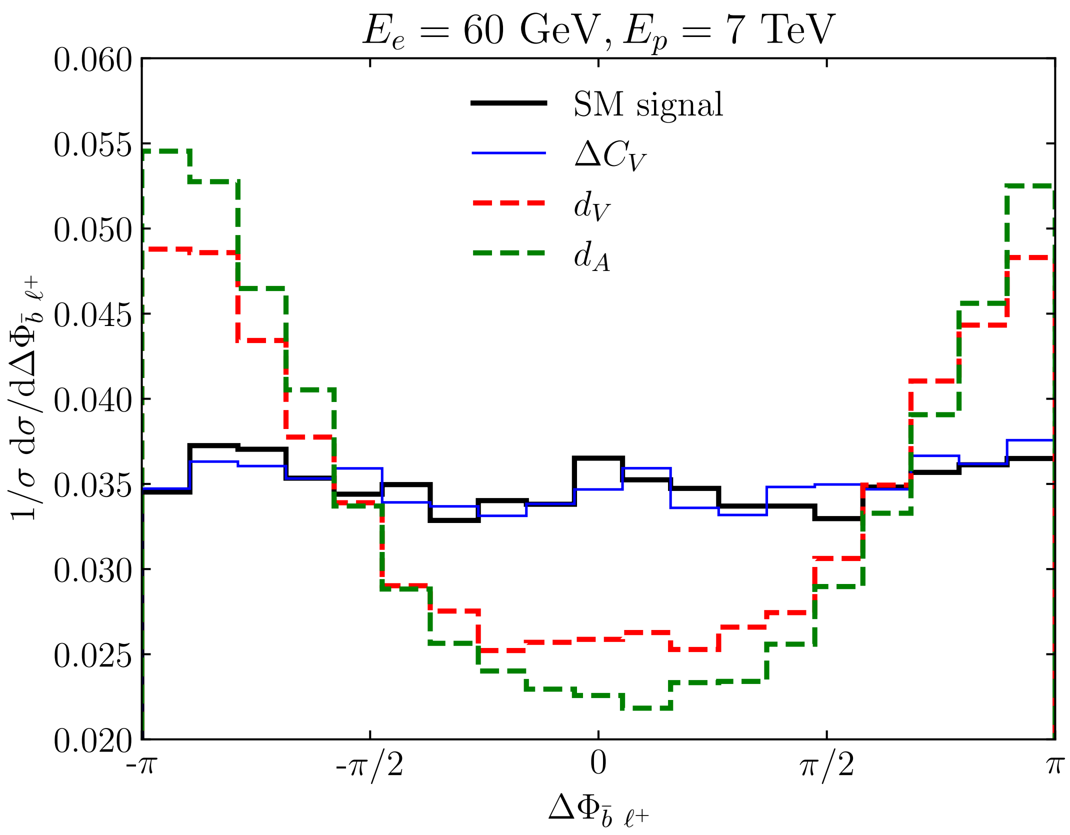

Analysis and Results:

photo-production: $\gamma p \to t\bar{t}$ [semi-leptonic top-decay]

$$\mathcal{L}_{t\bar{t}\gamma} = \left[-eQ_t\bar{t}\gamma^\mu(1+\Delta C_V)tA_\mu\right] + \left[-e\bar{t}\frac{i\sigma^{\mu\nu}q_\nu}{m_t}(d_V + id_A)tA_\mu\right]$$

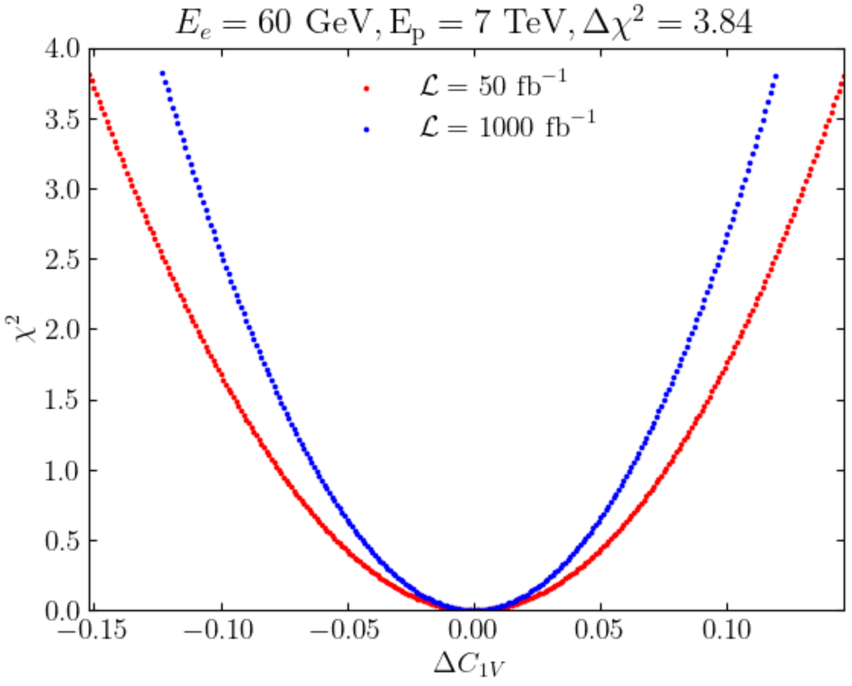

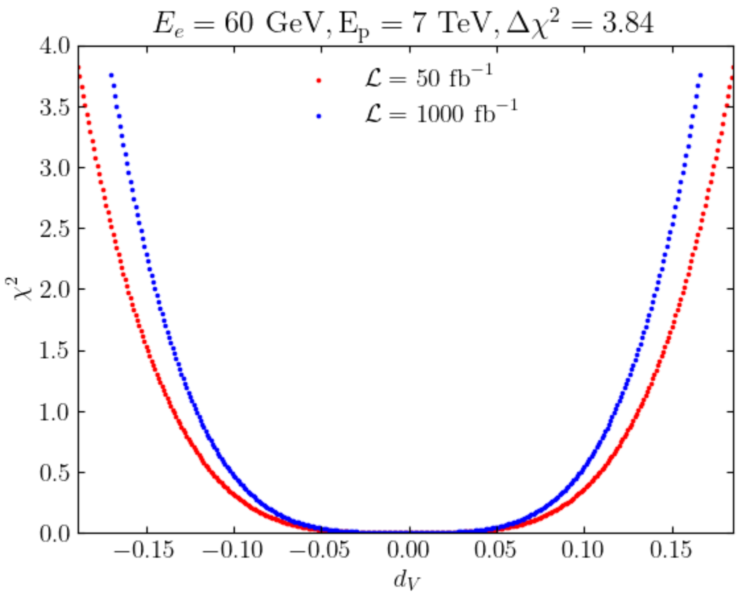

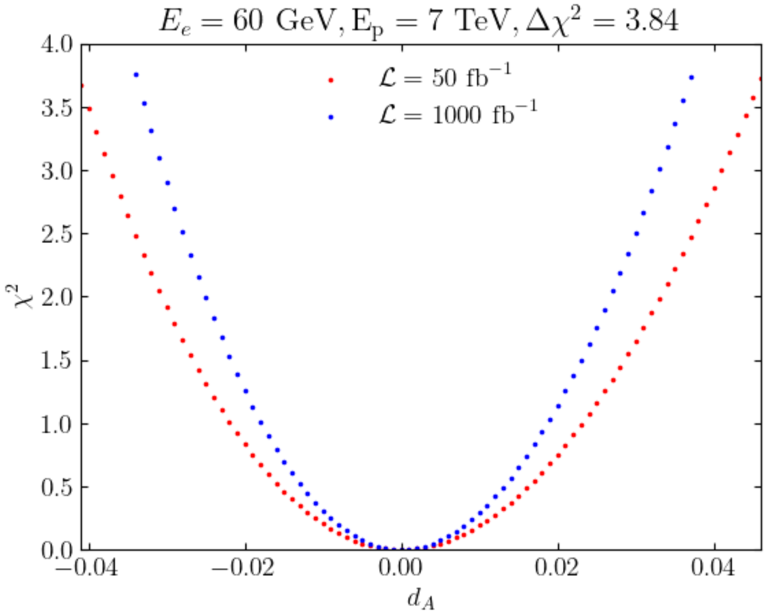

The χ^2 is defined as

$$\chi^2 = \sum_{k=1}^{n}\left(\frac{\sigma_k^{\mathrm{BSM}}(C_i) - \sigma_k^{\mathrm{exp}}}{\Delta\sigma_k}\right)^2,$$

Analysis and Results:

photo-production: $\gamma p \to t\bar{t}$ [semi-leptonic top-decay]

$$\mathcal{L}_{t\bar{t}\gamma} = \left[-eQ_t\bar{t}\gamma^{\mu}(1+\Delta C_V)tA_{\mu}\right]$$

$$+ \left[-e\bar{t}\frac{i\sigma^{\mu\nu}q_{\nu}}{m_t}(d_V + id_A)tA_{\mu}\right]$$

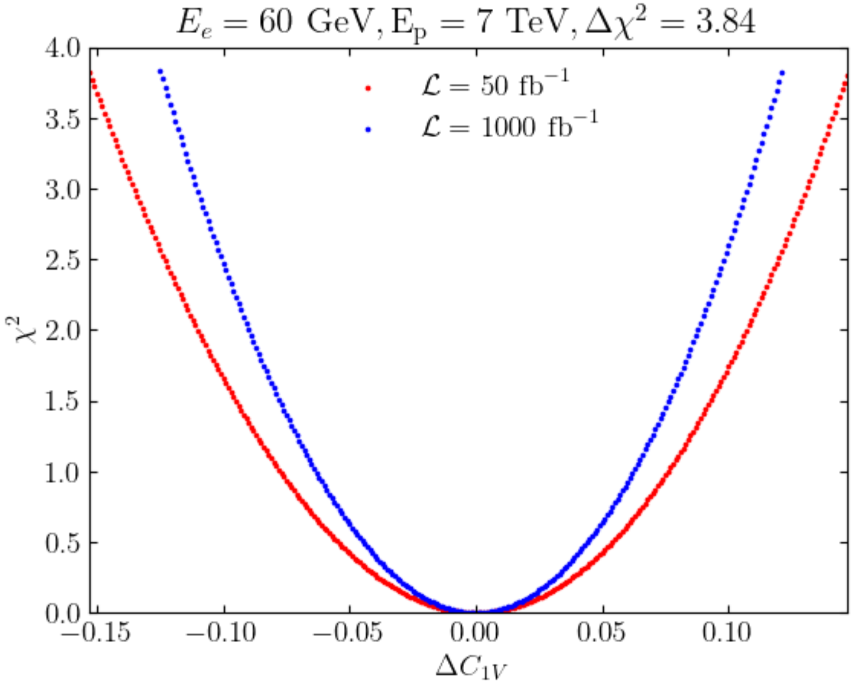

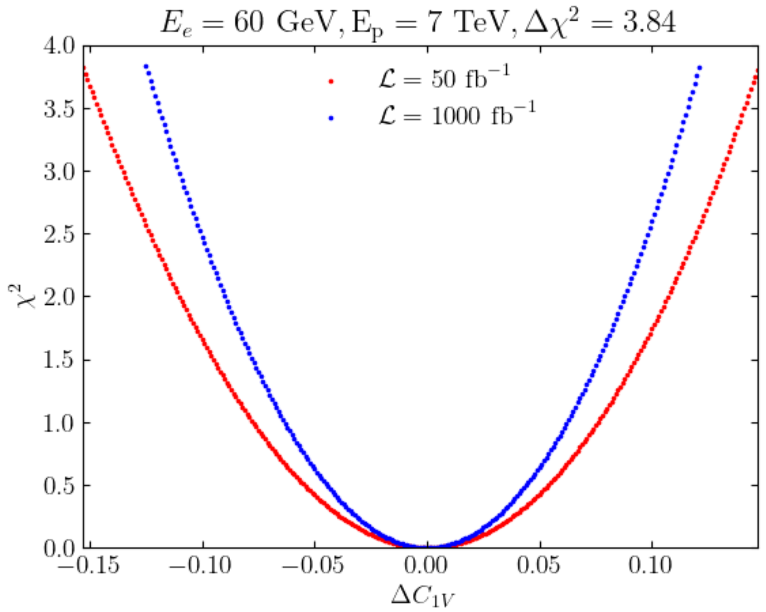

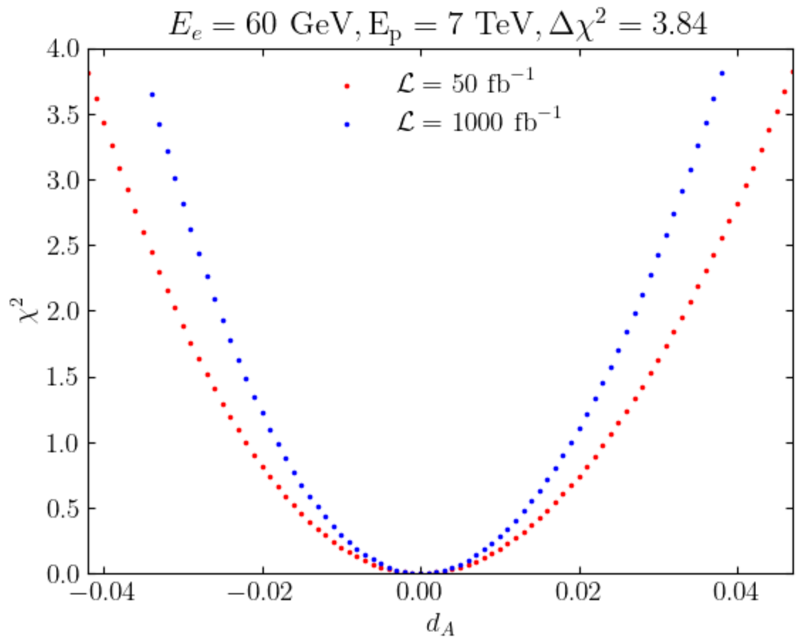

The χ^2 is defined as

$$\chi^2 = \sum_{k=1}^{n}\left(\frac{\sigma_k^{\mathrm{BSM}}(C_i) - \sigma_k^{\mathrm{exp}}}{\Delta\sigma_k}\right)^2,$$

photo-production: $\gamma p \to t\bar{t}$ [semi-leptonic top-decay]

Analysis and Results:

$$\mathcal{L}_{t\bar{t}\gamma} = \left[-eQ_t\bar{t}\gamma^{\mu}(1+\Delta C_V)tA_{\mu}\right] + \left[-e\bar{t}\frac{i\sigma^{\mu\nu}q_{\nu}}{m_t}(d_V+id_A)tA_{\mu}\right]$$

TABLE II. The 95% C.L. intervals for the BSM coupling parameters d_V and d_A, and SM correction term ΔC_V, with $\Lambda = 1$ TeV, extracted from a multi-bin χ^2 analysis of the $\Delta\phi$ distributions. Assuming $\delta_s = 5\%$, results from the one-parameter analysis are shown for $\mathcal{L} = 50$ fb^{-1} and 1000 fb^{-1}.

	Di-leptonic		Semileptonic (ℓ^-)		Semileptonic (ℓ^+)	
Coupling	50 fb^{-1}	1000 fb^{-1}	50 fb^{-1}	1000 fb^{-1}	50 fb^{-1}	1000 fb^{-1}
ΔC_{1V}	[-0.206, 0.195]	[-0.132, 0.128]	[-0.152, 0.146]	[-0.123, 0.119]	[-0.153, 0.147]	[-0.125, 0.121]
d_V	[-0.316, 0.323]	[-0.284, 0.291]	[-0.189, 0.185]	[-0.170, 0.166]	[-0.185, 0.187]	[-0.167, 0.168]
d_A	[-0.111, 0.156]	[-0.092, 0.119]	[-0.041, 0.046]	[-0.034, 0.037]	[-0.042, 0.047]	[-0.034, 0.038]

Results: Limits at 95% CL):

$$\mathcal{L}_{t\bar{t}\gamma} = \left[-eQ_t\bar{t}\gamma^{\mu}(1+\Delta C_V)tA_{\mu}\right] + \left[-e\bar{t}\frac{i\sigma^{\mu\nu}q_{\nu}}{m_t}(d_V+id_A)tA_{\mu}\right]$$

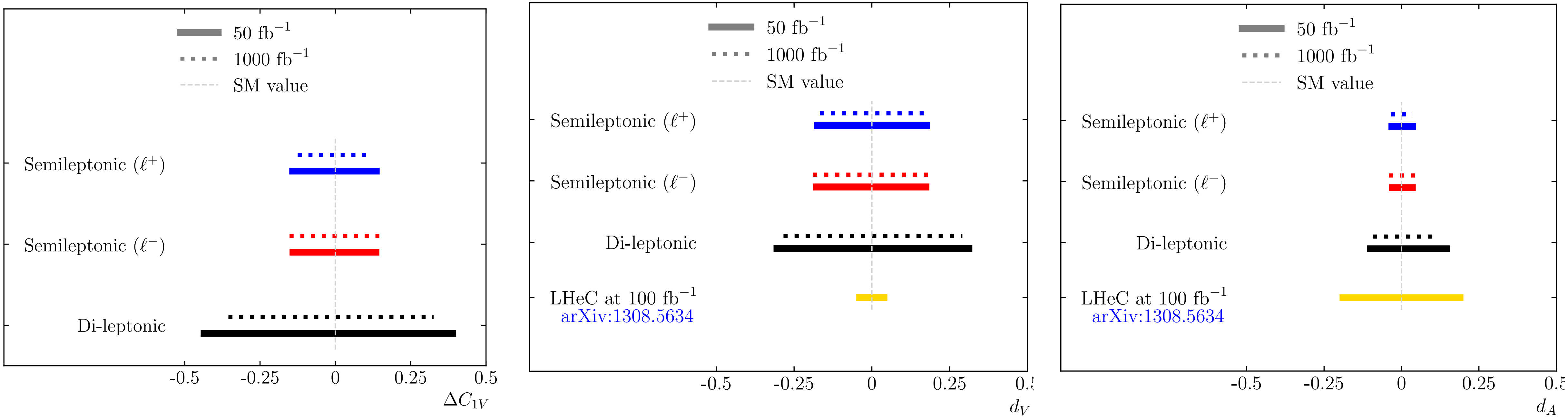

Conclusions and way forward:

- The differential analysis is used to probe the sensitivity of couplings in SM as well as BSM in the photo-production mode for di-leptonic and semi-leptonic decay channels.

- As the integrated luminosity increases from 50 fb^{-1} to 1000 fb^{-1}, the bounds on ΔC_{1V} improve by ~35% in the di-leptonic channel, and ~18% in the semi-leptonic channel,

- The bounds on d_V improve by ~10% for both decay channels when moving from 50 fb^{-1} to 1000 fb^{-1}, while d_A improves by ~21% and ~18.5% for the di-leptonic and semi-leptonic channels respectively.

- Compared to previous constraints as outlined in arXiv:1308.5634 obtained for LHeC @ 100 fb^{-1}, our constraints on d_V are ~84% times wider for the di-leptonic channel at both 50 fb^{-1} and 1000 fb^{-1} luminosities.

- In the semi-leptonic channel, our bounds on d_V are ~70% wider than the LHeC results for both luminosities.

Conclusions and way forward:

- On the hand, our constraints on d_A are more stringent than the ones reported for LHeC @ 100 fb^{-1}.
- At the integrated luminosity of 50 fb^{-1}, our limits are ~50% and 360% tighter than the LHeC limits for the di-leptonic channel and semileptonic channel respectively.
- At 1000 fb^{-1}, the limits on d_A are ~90% and ~460% tighter than the LHeC limits @100 fb^{-1} luminosity for the di-leptonic and semi-leptonic channels respectively.
- The study is currently in the preliminary stage and further investigation are underway.
- Various other observables such at the spin correlation and asymmetry of the top quarks are currently under consideration in order to improve the constraints on the coupling parameter.
- Correlation among the coupling parameters is under investigation (Correlation Matric).

Thank you!